P. Orlandi*, R. Verzicco* and G.J.F. van Heijst+

Stability of Shielded Vortex Dipoles

Abstract

In this study we consider a Lamb dipole and a shielded dipole with the same linear relationship between the vorticity ω and the stream function Ψ. In the second case the vorticity distribution is that of a Lamb dipole surrounded by an oppositely-signed vorticity layer. Direct simulations for moderate values of the Reynolds number have shown that the Lamb dipole maintains its structure while the shielded dipole breaks down. A numerical study of the evolution of small vorticity perturbations has shown that in the Lamb dipole the disturbance is convected far from the main structure, whereas in the shielded dipole the disturbance remains trapped within the vortical structure and grows in time.

Introduction

Vortex dipoles are common features of geophysical flows, and they are believed to play an important role in the general large-scale circulation, since they provide an important mechanism in the transport of various physical properties. In the ocean, dipolar vortices may be generated as a result of shedding from unstable coastal currents or due to localized wind forcing. In the atmosphere, dipolar flow structures may occur in the form of blocking systems which tend to have a stabilizing influence on the local weather. Within the context of the stability of such flow structures it is of importance to know whether the structure, once perturbed, relaxes towards its initial (stable) state. It is easy to show that any functional relationship $\omega = f(\Psi)$ between the vorticity ω and the stream function Ψ satisfies $J(\omega, \Psi) = 0$ and thus represents a stationary solution of the Euler equations. An interesting query is whether this functional relationship indicates stability or not.

In a previous study (Cavazza *et al.*, 1992) we considered the behaviour of a Lamb dipole (with $\omega = k^2\Psi$, see Lamb 1932) when subjected to different types of small perturbations (here we refer to the vortex structure as 'Lamb dipole', although the name 'Chaplygin-Lamb dipole' might be more appropriate, see Meleshko & van Heijst, 1994). In the numerical simulations it was observed that during the first stages of the flow evolution the dipole generally ejects patches of vorticity, while the finally remaining dipole attained a structure with the same

linear relationship but with a slope $k' = k/a'$, with a' the radius of the new dipole.

In the present study we address the question whether the linear relationship is the only condition necessary to show that the dipole has reached a stable state. To this purpose we have considered both the Lamb dipole and the shielded dipole, *i.e.* a Lamb dipole surrounded by an oppositely-signed vorticity layer. The stream functions Ψ and Ψ_S of the Lamb dipole and the shielded dipole, respectively, are given by

$$\Psi = -2U \frac{J_1(kr)}{kJ_0(ka)} \sin\theta, \qquad 0 \leqslant r \leqslant a \tag{1}$$

$$\Psi_S = -2U \frac{J_1(kr)}{kJ_0(kb)} \sin\theta, \qquad 0 \leqslant r \leqslant b \tag{2}$$

with U the translation velocity of the Lamb dipole, J_0 and J_1 the zeroth and first order Bessel functions of the first kind, respectively, and $ka = 3.832$ and $kb = 7.016$ the first and second zeros of J_1, respectively. The 'shield' of the shielded dipole lies in the ring $a \leqslant r \leqslant b$, and contains a dipolar vorticity distribution of polarity opposite to that of the dipole core $0 \leqslant r \leqslant a$. Although this shielded dipole is a solution of the stationary Euler equation, the numerical simulations to be described below indicate that this structure is unstable.

Numerical simulation

The stability of these vortex structures has been studied numerically by solving the vorticity equation

$$\frac{\partial\omega}{\partial t} + J(\omega, \Psi) = \frac{1}{Re}\nabla^2\omega \tag{3}$$

where J is the Jacobian operator and Re is the Reynolds number based on the dipole radius a and translation speed U. The numerical finite differences scheme has been described in Orlandi (1990) and Orlandi & van Heijst (1992), and its performance has been tested both by grid-refinement checks and by changing the location of the symmetry boundary conditions. Here it suffices to briefly describe the main characteristics of the numerical method. The system of equations is second order accurate in time and space, and the convective terms have been discretized by the Arakawa scheme (Arakawa, 1966) that conserves, in the inviscid limit, total energy and enstrophy, and maintains the skew symmetry of the Jacobian. This conservation property ensures not only the stability of the calculation but also the correct energy transfer. The advancement in time of the solution has been obtained by a third-order Runge-Kutta scheme calculating the nonlinear terms explicitly and the viscous terms implicitly. The large stability limit $CFL \leqslant \sqrt{3}$ allows a large Δt. Periodic boundary conditions in one direction

permit the use of FFT's and thus the stream function is obtained by a direct solver.

The calculations presented here were performed on a uniform 193×193 grid on the half-plane $-4.6 < x < 4.6$, $0 < y < 7$ (in view of the flow symmetry about $y = 0$), with periodic boundary conditions in the x-direction.

Apart from the numerical simulations of the regular and shielded Lamb dipoles given by (1) and (2), respectively, additional simulations were performed in which the dipolar vortex structures were locally perturbed in the area of maximum vorticity gradients, *i.e.* in a narrow band along the radius $r = a$. This vorticity perturbation, that is superimposed on the basic vorticity distribution, was taken as

$$\omega'(r, \theta) = \varepsilon \exp\left\{-\frac{(1 - r/a)^2}{\sigma^2}\right\} \sin 4\theta, \tag{4}$$

with ε the perturbation amplitude and σ a parameter that controls the width of the perturbation band around $r = a$. The amplitude ε was set at a nondimensional value $\varepsilon = 0.05$, which is small compared to the peak value 11.08 of the unperturbed Lamb dipole, whereas the width parameter was set at $\sigma = 0.15$. The structure of the vorticity perturbations of the unshielded and shielded dipoles are shown in Figure 1.

Results

The numerical solution of (3) for the Lamb dipole with the initial stream function (1) revealed that the dipole maintains its shape for a long time and that,

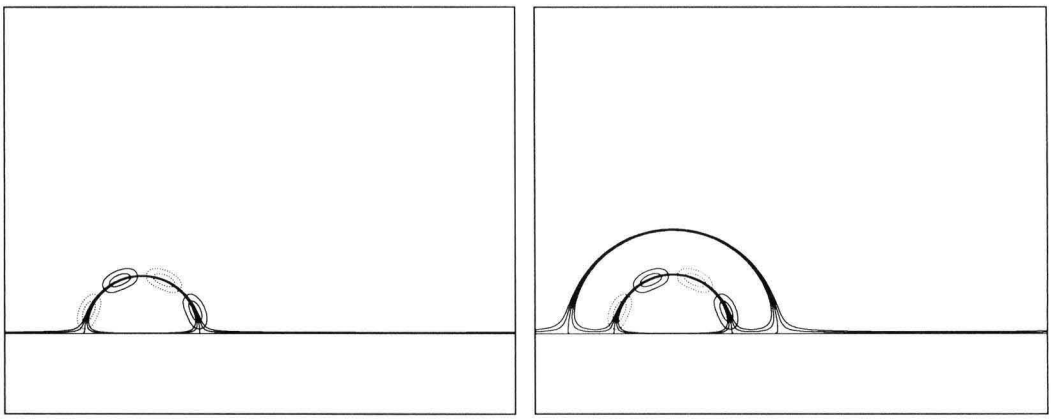

Fig. 1. Graphs showing the distribution of the initial perturbation vorticity (—— positive, ... negative) for (a) the regular and (b) the shielded Lamb dipole (only the upper halves $0 \leqslant \theta \leqslant \pi$ are shown). The structure of the dipoles is shown by the unperturbed separatrices and a few neighbouring streamlines.

Fig. 2. The evolution of the unperturbed Lamb dipole for $Re = 1000$ from $t = 0$ to $t = 5$ (in non-dimensional time units) shown by vorticity contours $\Delta\omega = 0.5$; only the upper half-plane is shown.

depending on the Reynolds number, the peak vorticity decreases in time. Some results for $Re = 1000$ are shown in Figure 2: at $t = 5$ (the time is scaled with U and 2a) has travelled approximately 5 dipole diameters and the cusp-shaped vorticity contour indicates a distortion of the initial dipole structure in the wake, *i.e.* near the rear stagnation point. In contrast, the shielded vortex loses its original shape very quickly, see Figure 3. In comparison with the unshielded dipole, the structure shows an initial tendency to move in opposite direction. This may be surprising at first glance, but in fact it is explicitly given by the solutions (1) and (2) which have different signs since $J_0(ka) = -0.4027...$ and $J_0(kb) = +0.3001...$

The other vorticity patch is seen to be split into two parts, one being left behind near the symmetry axis, while the other pairs with the original positive core patch in order to form an asymmetric dipole that slowly moves away from the symmetry axis. This behaviour may be understood from the fact that the net negative vorticity contained in the shell is larger than that in the positive core. Besides, the position of extreme negative vorticity in the shell lies closer to the vorticity maximum in the positive core half than that of the negative core half. Apparently, the combination of these effects leads to a redistribution of the vorticity in the outer band and a separation of both inner core halves. From these simulations it thus appears that the outer band of oppositely-signed vorticity is

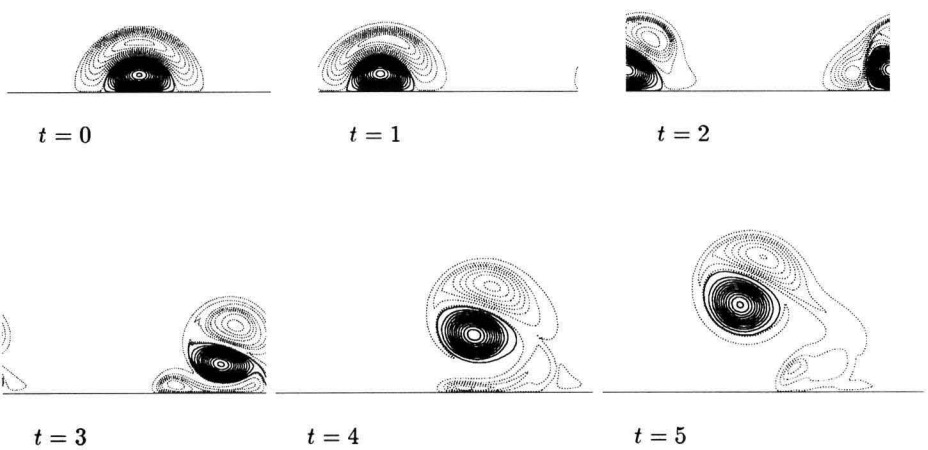

Fig. 3. The evolution of the unperturbed shielded dipole for $Re = 1000$ from $t = 0$ to $t = 5$ shown by vorticity contours $\Delta\omega = \pm 0.5$ (—— positive, ... negative); only the upper half-plane is shown.

not just a passive shield around the dipolar core: the outer vorticity shell is dynamically important and affects the behaviour of the dipole core to a high degree.

In order to gain some insight in the behaviour of the shielded dipole in comparison with that of the regular dipole, we studied the evolution of the vorticity perturbation (4) by numerically solving the 'linearized' vorticity equation

$$\frac{\partial \omega'}{\partial t} + J(\omega', \Psi_0) + J(\omega_0, \Psi') = \frac{1}{Re} \nabla^2 \omega' \tag{5}$$

in which the prime denotes perturbation quantities, whereas the subscript 0 refers to the nonperturbed dipole solutions (1) and (2). The calculations have been performed for $Re = 5000$, so for the case of slight viscosity. The distributions of the perturbation vorticity after 15 time units for both the regular and the shielded dipole are shown in Figure 4. For the Lamb dipole, a considerable portion of the perturbation vorticity is expelled, and thus dissipated in the wake, while only some weak effects of the perturbation remain in the dipole's interior. In contrast, in the case of the shielded dipole most of the perturbation vorticity remains trapped within the structure, see Figure 4b, while only a negligible amount is left behind in the wake. Moreover, one observes the formation of larger regions of positive and negative ω' within the two recirculation regions of the shielded dipole half, thus resulting in an increased distorting effect. This remarkable difference in the evolution of the perturbation vorticity may give a clue to the observed instability of the shielded dipole, see Figure 3.

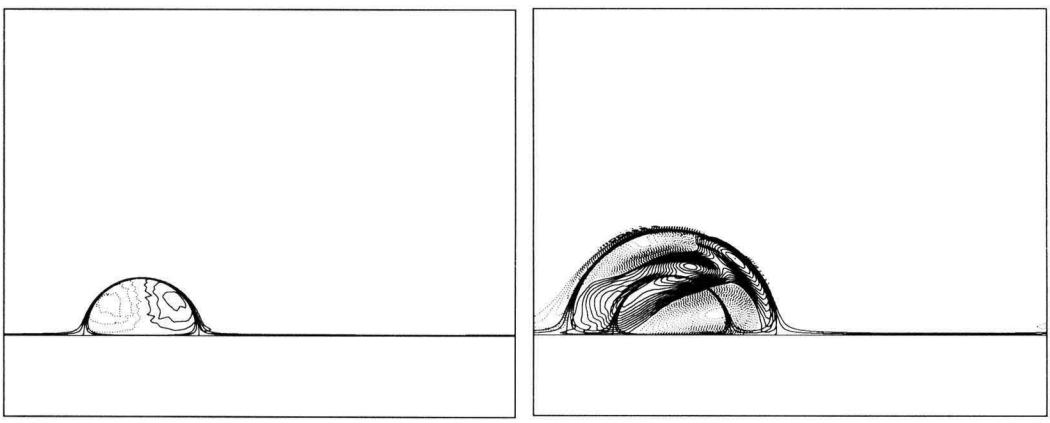

Fig. 4. The distribution of the perturbation vorticity at $t = 15$ for (a) the regular dipole and (b) the shielded dipole. The structure of the unperturbed dipole is shown by the unperturbed streamlines as in Figure 1.

Discussion

The numerical simulations of the regular and shielded dipoles have shown remarkable differences in their evolution. In order to gain insight in the flow evolution it is useful to consider the topological flow structure of both dipoles. As schematically shown in Figure 5, the topological structure of the Lamb dipole is characterized by a circular separatrix Ψ_a and two stagnation points (*i.e.* hyperbolic points) at the intersections of the separatrix and the symmetry streamline $\Psi_{0,\pi}$. The shielded dipole has an outer separatrix Ψ_b with two stagnation points S_{b_1} and S_{b_2}, and an inner separatrix Ψ_a with stagnation points S_{a_1} and S_{a_2}. It is known from previous studies on a perturbed point-vortex dipole, which has the same topology, that small perturbations introduced inside or at the separatrix generally result in the 'opening' of the dipole atmosphere at the rear stagnation point, here S_{a_2} (*cf.* Rom-Kedar *et al.* 1990 and Velasco Fuentes & van Heijst 1994). In general this results in fluid exchange between the dipole interior and the exterior, *i.e.* in detrainment and entrainment at the dipole's rear. Most likely this mechanism is responsible for the effective 'leaking' of the perturbation vorticity ω' from the Lamb dipole interior, as observed in the numerical simulation (see Figure 4a). As indicated in Figure 5b, the topological structure of the shielded dipole is essentially different: any small perturbations introduced near the inner separatrix Ψ_a will quickly leak into the outer shell (near the inner stagnation point S_{a_1}) according to the same mechanism as described above. The recirculation in the outer shell results in a quick spreading of the perturbation vorticity over the entire vortex domain (see Figure 4b), while initially hardly any mass exchange between the dipole and its exterior occurs. Obviously, internal perturbations remain trapped within the shielded dipole, thus leading to changes in the internal vorticity structure. This internal redistribution mechanism is most likely the reason for the break-up of the shielded dipole as observed in the simulations (Figure 3). Although these simulations were carried out for an unperturbed shielded dipole, it may be expected that diffusion of vorticity (being most effective at locations of maximum vorticity gradients, *i.e.* at both separatrices) results in a similar perturbation vorticity field as described artificially by (4).

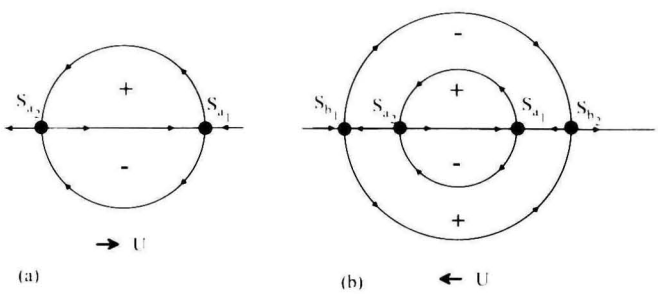

Fig. 5. Schematic drawing of the topological inviscid flow structure of (a) the Lamb dipole and (b) the shielded dipole, seen in a frame co-moving with velocity U.

In view of their different evolutions, the question arises whether the regular Lamb dipole and the shielded dipole possibly contain different amounts of *enstrophy*. The enstrophy is here

$$G = \int\int \frac{1}{2}\omega^2 \, dA = \frac{1}{2}k^4 \int_o^{2\pi} \int_o^R \Psi^2 r \, dr \, d\theta, \tag{6}$$

with R the dipole radius and Ψ the stream function given by (1) or (2). The integrals are easily evaluated, and one derives (with the index S referring to the shielded dipole):

$$G = \pi a^2 k^2 U^2, \qquad G_S = \pi b^2 k^2 U^2. \tag{7}$$

Although the *total* enstrophy of the shielded dipole is larger than the total enstrophy of the Lamb dipole by a factor of $(b/a)^2 \simeq 3.37$, the enstrophy *per unit area* is the same for both vortex structures:

$$G' = \frac{G}{\pi a^2} = k^2 U^2, \qquad G'_S = \frac{G_S}{\pi b^2} = k^2 U^2. \tag{7}$$

Apparently, this does not provide any further clues. Figure 6 shows the evolution of G' and G'_S as calculated numerically for $Re = 1000$ (the corresponding evolutions of the spatial vorticity distribution are presented in Figures 2 and 3). Both G' and G'_S show a gradual decrease, although G'_S decreases at a higher rate. The decrease of the enstrophy is entirely due to the removal of weak, small-scale low-amplitude vorticity (less than 10^{-6}) in the exterior flow field during the numerical simulations. The different decay rates indicate that the slightly viscous Lamb dipole shows only little 'leaking' of vorticity in comparison with the shielded dipole, which by breaking up soon loses its coherent character.

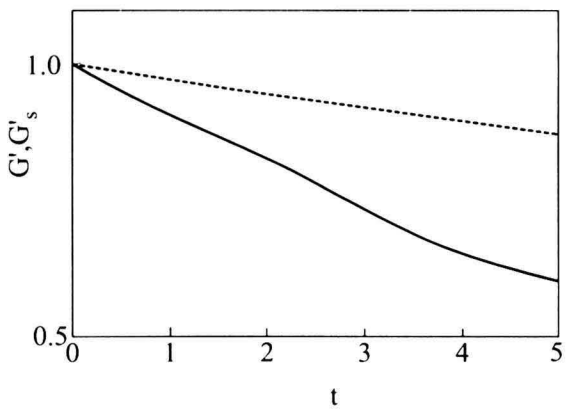

Fig. 6. Evolution of the enstrophies G' and G'_S calculated numerically for $Re = 1000$. The dotted curve represents the Lamb dipole (G'), while the solid curve represents the shielded dipole (G'_S).

Conclusions

In this numerical study we have provided evidence that the shielded Lamb dipole, although governed by the same linear relationship between the vorticity and the stream function as the regular Lamb dipole, is unstable for moderate values of the Reynolds number. It is believed that the explanation for this instability lies in the flow topology of the vortex structure: small internal vorticity perturbations (either artificially generated or arising from diffusion of vorticity) are seen to remain trapped within the shielded dipole, whereas they are quickly detrained in the case of a regular Lamb dipole.

References

Arakawa, A., 1966 - Computational design for long term numerical integration of the equations of fluid motion: Two-dimensional incompressible flow. Part I. *J. Comput. Phys.* **1**, 119–143.

Cavazza, P., G.J.F. van Heijst & P. Orlandi, 1992 - The stability of vortex dipoles. Proc. 11^{th} Australasian Fluid Mech. Conf., Hobart, Australia.

van Heijst, G.J.F., R.C. Kloosterziel & C.W.M. Williams, 1991 - Laboratory experiments on the tripolar vortex in a rotating fluid. *J. Fluid Mech.* **225**, 301–331.

Lamb, H., 1932 - *Hydrodynamics*. Cambridge University Press.

Meleshko, V.V. & G.J.F. van Heijst, 1994 - On Chaplygin's investigations of two-dimensional vortex structures in an inviscid fluid. *J. Fluid Mech.* **272**, 157–182.

Orlandi, P., 1990 - Vortex dipole rebound from a wall. *Phys. Fluids* **A2**, 1429–1436.

Orlandi, P. & G.J.F. van Heijst, 1992 - Numerical simulations of tripolar vortices in 2D flows. *Fluid Dyn. Res.* **9**, 179–206.

Rom-Kedar, V., A. Leonard & S. Wiggins, 1990 - An analytical study of transport, mixing and chaos in an unsteady vortical flow. *J. Fluid Mech.* **214**, 347–394.

Velasco Fuentes, O.U., G.J.F. van Heijst & B.E. Cremers, 1994 - Chaotic advection by dipolar vortices on a β-plane. *J. Fluid Mech.* (submitted.) Also: B.E. Cremers & O.U. Velasco Fuentes, 1994 - Chaotic advection by dipolar vortices on a β-plane. *This issue*.

* Università di Roma "La Sapienza"
Dipartimento di Meccanica e Aeronautica
Via Eudossiana 18, 00184 Rome, Italy

\+ Fluid Dynamics Laboratory
Eindhoven University of Technology
P.O. Box 513, 5600 MB Eindhoven, The Netherlands